

# The first structurally characterized, quadruple-bonded complexes containing chiral amine ligands; syntheses, structures and optical activities of $[\text{Mo}_2\text{Cl}_4(\text{S-chea})_4]$ and $[\text{Mo}_2\text{Cl}_4(\text{R-chea})_4]$ (chea = 1-cyclohexylethylamine) †

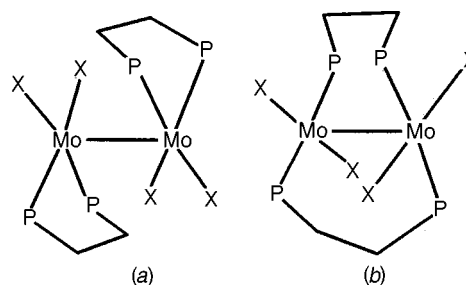
Huey-Lin Chen,<sup>a</sup> Chang-Tai Lee,<sup>a</sup> Chun-Ting Chen,<sup>a</sup> Jhy-Der Chen,<sup>\*,a</sup> Lin-Shu Liou<sup>b</sup> and Ju-Chun Wang<sup>b</sup>

<sup>a</sup> Department of Chemistry, Chung-Yuan Christian University, Chung-Li, Taiwan, Republic of China

<sup>b</sup> Department of Chemistry, Soochow University, Taipei, Taiwan, Republic of China

The complexes  $[\text{Mo}_2\text{Cl}_4(\text{S-chea})_4]$  **1** (chea = 1-cyclohexylethylamine) and  $[\text{Mo}_2\text{Cl}_4(\text{R-chea})_4]$  **2** were prepared by reactions of  $[\text{Mo}_2\text{Cl}_4(\text{PPh}_3)_2(\text{MeOH})_2]$  with *S*- and *R*-chea, respectively, in acetone. Their NMR, UV/VIS and circular dichroism spectra have been recorded and the structures of both **1** and **2** have been determined. The molybdenum atoms in both crystal structures were found to be disordered, so that while only one set of ligand atoms can be resolved, there are two incompletely occupied sets of metal atoms. The ratios of the primary to the secondary form are 97:3 and 94:6 for **1** and **2**, respectively. The lowest-energy bands of the absorption spectra at 531 nm for both **1** and **2** can be assigned to  $\delta_{xy} \rightarrow \delta_{xy}^*$  transitions. The solid-state CD spectra of these two complexes show two prominent bands at 520 and 455 nm and form mirror images of each other. The variable-temperature CD spectra of the complexes in toluene intersect in isosbestic points, indicating temperature-dependent equilibria between pairs of conformers for each complex. The Wood-Fickett-Kirkwood method has been used to calculate the free-energy changes of the  $\Delta$  and  $\Lambda$  conformers and their populations in solution.

The optical activities of quadruply bonded complexes of the type  $\text{Mo}_2\text{X}_4(\text{L-L})_2$  (X = Cl or Br, L-L = diphosphine ligand) have been the subject of several studies during recent years.<sup>1</sup> The complexes were shown to be capable of existing in two isomeric forms,  $\alpha$  and  $\beta$ , shown schematically in Scheme 1. Two types of chiral complexes of the form  $\beta\text{-Mo}_2\text{X}_4(\text{L-L})_2$  have been structurally characterized. The first type has 'class I' chromophores,<sup>2</sup> that is inherently chiral chromophores due to ligand constraint, and their CD spectra can be explained by the CD sign rule,<sup>3</sup> which has been verified with the syntheses and structural characterization of the complexes  $\beta\text{-}[\text{Mo}_2\text{X}_4(\text{S,S-dppb})_2]$  [X = Cl or Br; *S,S*-dppb = (2*S*,3*S*)-bis(diphenylphosphino)butane],<sup>4</sup>  $\beta\text{-}[\text{Mo}_2\text{Cl}_4(\text{S,S-diop})_2]$  [*S,S*-diop = (+)-4,5-bis(diphenylphosphinomethyl)-2,2-dimethyl-1,3-dioxolane] and  $\beta\text{-}[\text{Mo}_2\text{Cl}_4(\text{R,R-diop})_2]$  [*R,R*-diop = (-)-4,5-bis(diphenylphosphinomethyl)-2,2-dimethyl-1,3-dioxolane].<sup>5</sup> The other type of chiral complex has 'class II' chromophores,<sup>2</sup> that is an intrinsically achiral chromophore which displays chiroptical effects through perturbation by chiral surroundings. The chiral complexes  $\beta\text{-}[\text{Mo}_2\text{Cl}_4(\text{S,S-bppm})_2]$  [*S,S*-bppm = (2*S*,4*S*)-*N*-(*tert*-butoxycarbonyl)-4-(diphenylphosphino)-2-(diphenylphosphinomethyl)pyrrolidine]<sup>6</sup> and  $\beta\text{-}[\text{Re}_2\text{Cl}_6(\text{S,S-isidiop})]$  (isidiop = a rearranged form of diop),<sup>7</sup> which have a torsional angle of approximately 0°, appear to belong to this category. The one-electron static coupling mechanism<sup>6,7</sup> was invoked to explain the CD spectrum for these complexes. Recently, the optical activities of the chelating complexes  $\alpha\text{-}[\text{Mo}_2\text{Cl}_4(\text{R,R-Me-Duphos})_2]$  {*R,R*-Me-Duphos = 1,2-bis[(2*R*,5*R*)-2,5-dimethylphospholan-1-yl]benzene} and  $\alpha\text{-}[\text{Mo}_2\text{Cl}_4(\text{S,S-Me-Duphos})_2]$  {*S,S*-Me-Duphos = 1,2-bis[(2*S*,5*S*)-2,5-dimethylphospholan-1-yl]benzene} have been reported and the structure of  $\alpha\text{-}[\text{Mo}_2\text{Cl}_4(\text{R,R-Me-Duphos})_2]$  has been determined by X-ray crystallography.<sup>8</sup> Both the solution and solid CD spectra



**Scheme 1** Drawings of the structures of the  $\alpha$  (a) and  $\beta$  (b) isomers of  $\text{Mo}_2\text{X}_4(\text{L-L})_2$  complexes

of these two complexes showed opposite phases to those expected by the CD sign rule. Since the  $\alpha$ -form complexes have no ligand constraints that limit the rotation of the M-M bond contrary to  $\beta$ -form complexes, it is possible that the configurations and magnitudes of the average twist angle in solution are not the same as those obtained in the crystal.<sup>8</sup> Optical activities of several chiral complexes containing diamine ligands, such as  $[\text{Mo}_2(\text{R-pn})_4]^{4+}$  (pn = 1,2-diaminopropane),<sup>9</sup>  $[\text{Mo}_2(\text{S,S-bn})_4]^{4+}$  (bn = 2,3-diaminobutane)<sup>10</sup> and  $[\text{Mo}_2\text{Cl}_4(\text{R,R-dach})_2]$  (dach = 1,2-diaminocyclohexane)<sup>11</sup> have been reported, and on the basis of the spectroscopic and elemental analysis results they are all assigned as bridged complexes.

To compare the optical activities of complexes of the type  $\text{Mo}_2\text{X}_4\text{L}_4$ , where L is a monodentate ligand, with those of the two types of complexes containing bridging or chelating bidentate ligands mentioned above, we have prepared and studied  $[\text{Mo}_2\text{Cl}_4(\text{S-chea})_4]$  and  $[\text{Mo}_2\text{Cl}_4(\text{R-chea})_4]$  (chea = 1-cyclohexylethylamine). They are the first structurally characterized, quadruply bonded complexes containing chiral amine ligands. The preparations, structures and optical activities of these chiral complexes form the subject of this report.

† Non-SI unit employed: cal = 4.184 J.

## Experimental

### General procedures

All manipulations were carried out under dry, oxygen-free nitrogen by using Schlenk techniques, unless otherwise noted. Solvents were dried and deoxygenated by refluxing over the appropriate reagents before use. Methanol was purified by distillation from magnesium, *n*-hexane from sodium–benzophenone, and acetone and dichloromethane from  $P_2O_5$ . The visible absorption spectra were recorded on a Hitachi U-2000 spectrophotometer, circular dichroism (CD) spectra on an Aviv 62A DS spectrometer, mass spectra on a JEOL JMS-SX/SX 102 A spectrometer and NMR spectra on a Bruker 500 MHz spectrometer.

### Materials

The complex  $[Mo_2Cl_4(PPh_3)_2(MeOH)_2]$  was prepared according to a previously reported procedure.<sup>12</sup> The reagents *R*-(–)- and *S*-(+)-1-cyclohexylethylamine were from Aldrich Chemical Co.

### Preparations

**$[Mo_2Cl_4(S\text{-chea})_4]$  1 and  $[Mo_2Cl_4(R\text{-chea})_4]$  2.** The complex  $[Mo_2Cl_4(PPh_3)_2(MeOH)_2]$  (1 g, 1.08 mmol) and *S*-chea or *R*-chea (0.63 cm<sup>3</sup>, 4.32 mmol) were placed in a flask containing acetone (25 cm<sup>3</sup>). The mixture was then stirred at room temperature for 26 h to yield a red solid and a red solution. The solid was filtered off, washed with acetone and then dried under reduced pressure. Yield: 0.49 g (53.8%) for **1** and 0.50 g (54.9%) for **2**. UV/VIS (toluene): **1**, 531 nm. Mass spectrum (FAB): *m/z* (relative intensity, ion) 842 (3,  $M^+$ ), 715 (9,  $M^+ - \text{chea}$ ), 588 (9,  $M^+ - 2 \text{ chea}$ ), 460 (8,  $M^+ - 3 \text{ chea}$ ), 333 (5,  $M^+ - 4 \text{ chea}$ ) and 307 (100,  $Mo_2Cl_3^+$ ); **2**, 842 (7,  $M^+$ ), 715 (22,  $M^+ - \text{chea}$ ), 588 (22,  $M^+ - 2 \text{ chea}$ ), 460 (8,  $M^+ - 3 \text{ chea}$ ), 333 (6,  $M^+ - 4 \text{ chea}$ ) and 307 (100,  $Mo_2Cl_3^+$ ) (Found for **1**: C, 45.70; H, 8.07; N, 6.42. Found for **2**: C, 45.32; H, 8.02; N, 6.43. Calc. for  $C_{32}H_{68}Cl_4Mo_2N_4$ : C, 45.61; H, 8.13; N, 6.65%).

### X-Ray crystallography

Crystals suitable for X-ray diffraction were obtained by the slow diffusion of hexane into a  $CH_2Cl_2$  solution of complex **1** or **2**. The diffraction data for **1** and **2** were collected at 25 °C on a Siemens CCD diffractometer, which was equipped with graphite-monochromated Mo-K $\alpha$  ( $\lambda_a = 0.71073 \text{ \AA}$ ) radiation. Data reduction was carried by standard methods with use of well established computational procedures.<sup>13</sup> Basic information pertaining to crystal parameters and structure refinement is summarized in Table 1.

A red crystal of  $[Mo_2Cl_4(S\text{-chea})_4]$  or  $[Mo_2Cl_4(R\text{-chea})_4]$  was mounted on the top of a glass fiber with epoxy cement. The hemisphere data-collection method was used to scan the data points at  $2\theta < 47^\circ$ . The structure factors were obtained after Lorentz-polarization corrections. The positions of the heavy atoms, including two molybdenum atoms, were located by the direct method. The remaining atoms were found in a series of alternating Fourier-difference maps and least-square refinements.<sup>14</sup> The final residuals of the first refinement were  $R = 0.0581$ ,  $R' = 0.0593$  with the *R* configuration for the ligands for  $[Mo_2Cl_4(S\text{-chea})_4]$ . An inversion of coordinates to give the *S* configuration was made and the structure refined to convergence with  $R = 0.0576$ ,  $R' = 0.0585$ . The results clearly confirmed that the *S* isomer was indeed correct. For the complex  $[Mo_2Cl_4(R\text{-chea})_4]$  the final residuals were  $R = 0.0577$ ,  $R' = 0.0611$  with the *R* configuration for the ligands. Inversion to the *S* configuration gave  $R = 0.0582$  and  $R' = 0.0618$ .

CCDC reference number 186/775.

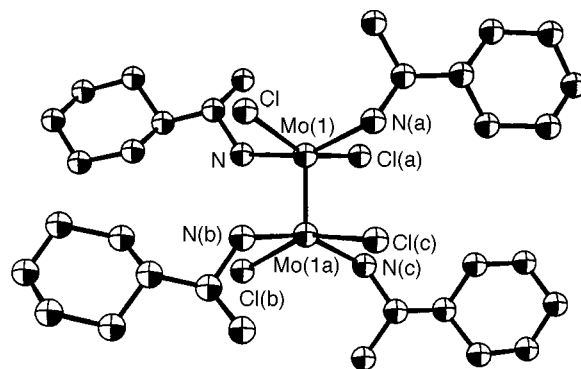


Fig. 1 An ORTEP drawing of the primary form of  $[Mo_2Cl_4(S\text{-chea})_4]$

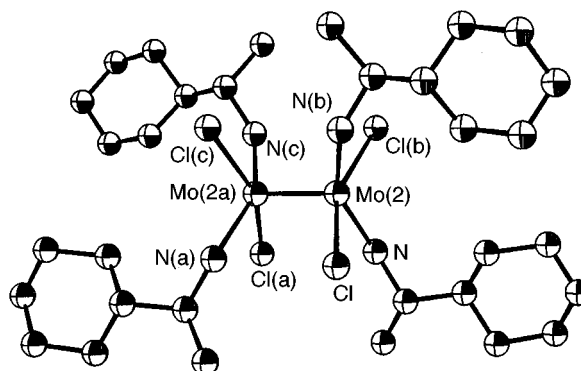


Fig. 2 An ORTEP drawing of the secondary form of  $[Mo_2Cl_4(S\text{-chea})_4]$

## Results and Discussion

### Syntheses and structural characterization

The red complexes  $[Mo_2Cl_4(S\text{-chea})_4]$  **1** and  $[Mo_2Cl_4(R\text{-chea})_4]$  **2** were prepared by reactions of  $[Mo_2Cl_4(PPh_3)_2(MeOH)_2]$  with *S*- and *R*-chea, respectively, in acetone. The mass spectra of the complexes show similar fragmentation patterns and abundances. Both contain peaks assignable to parent ions,  $M^+$ . The other fragment ions were produced by sequential loss of amine ligands but the losses of the chloride ions are not prominent. The most abundant ion is  $Mo_2Cl_3^+$ . Similar to the mass spectra reported for  $[Mo_2Cl_4(PMe_3)_4]$  and  $[W_2Cl_4(PMe_3)_4]$ ,<sup>15</sup> rupture of the metal–metal bond is not a major process.

Red crystals of both complexes **1** and **2** conform to the space group  $I222$  with two molecules in a unit cell. The complexes appear to be the first chiral ones of the type  $Mo_2X_4L_4$  ( $X = \text{halogen atom}$ ;  $L = \text{monodentate ligand}$ ) that have been structurally characterized. Their structures show two molecules, which have different chiralities, partially occupying a given site. Figs. 1 and 2 show ORTEP<sup>16</sup> diagrams for the primary and secondary form of **1**, respectively. The molecules have  $D_2$  symmetries and the Mo–Mo vectors lie along the two-fold axes. Although complexes **1** and **2** are not isostructural with  $[Mo_2Cl_4(PMe_3)_4]$ ,<sup>15</sup> these molecules have similar geometry that is typical of  $Mo_2X_4L_4$  complexes. Table 2 lists selected bond distances and angles for complexes **1** and **2**. Clearly, the values of these two enantiomeric molecules are nearly identical. The Mo–Mo bond distances of the primary form of complex **1** are 2.127(4) and 2.127(1) Å and those of the secondary form are 2.121(4) and 2.123(1) Å, respectively. These distances are similar to those of many analogous compounds that possess an Mo–Mo quadruple bond.<sup>1</sup> Noticeably, they are similar to that [2.144(5) Å] of the complex  $[Mo_2I_4(NCPh)_4]$ , where the organic ligands are co-ordinated to the Mo atoms through the nitrogen atoms.<sup>17</sup>

Fig. 3 shows an ORTEP diagram of complex **1** including both the primary and secondary forms. The two Mo–Mo vectors are clearly perpendicular to each other. The ratios of

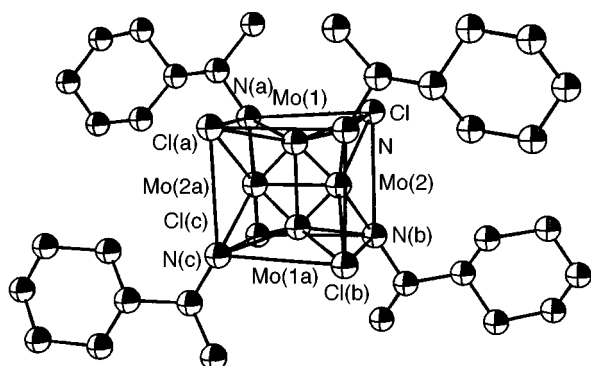
**Table 1** Crystal data for  $[\text{Mo}_2\text{Cl}_4(\text{S-chea})_4]$  **1** and  $[\text{Mo}_2\text{Cl}_4(\text{R-chea})_4]$  **2**\*

	<b>1</b>	<b>2</b>
$a/\text{\AA}$	6.899(1)	6.900(1)
$b/\text{\AA}$	15.594(3)	15.588(3)
$c/\text{\AA}$	19.296(4)	19.278(4)
$U/\text{\AA}^3$	2076(1)	2073(1)
$D/g\text{ cm}^{-3}$	1.348	1.350
Crystal size/mm	$0.05 \times 0.15 \times 0.5$	$0.1 \times 0.3 \times 0.4$
$\mu(\text{Mo-K}\alpha)/\text{mm}^{-1}$	0.886	0.887
No. orientation reflections	1485	1484
$2\theta$ Range/ $^\circ$	<46.58	<46.47
Data collection range ( $2\theta/^\circ$ )	3.36–46.58	3.36–46.47
No. unique data	1485	1484
No. observed data [ $F > 6.0\sigma(F)$ ]	789	790
No. parameters refined	98	99
$R$	0.0576	0.0577
$R'$	0.0585	0.0611
Quality-of-fit indicator	1.30	1.40
Largest shift/e.s.d., final cycle	0.010	0.10
Largest peak/e $\text{\AA}^{-3}$	0.91	0.72

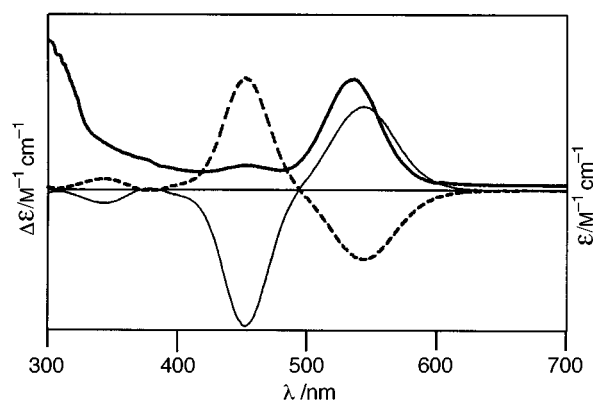
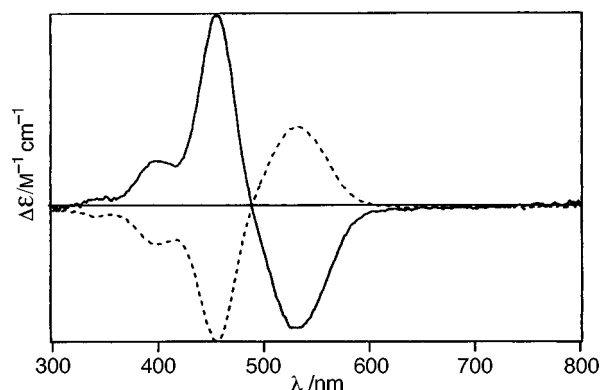
\* Details in common:  $\text{C}_{32}\text{H}_{68}\text{Cl}_4\text{Mo}_2\text{N}_4$ ,  $M$  842.6, orthorhombic, space group  $I222$ ;  $Z = 2$ ;  $R = \Sigma||F_o| - |F_c||/\Sigma|F_o|$ ;  $R' = [\Sigma w(|F_o| - |F_c|)^2/\Sigma w|F_o|^2]$ ;  $w = 1/[\sigma^2(F_o) + gF_o^2]$ ; quality of fit =  $[\Sigma w(|F_o| - |F_c|)^2/(N_{\text{observed}} - N_{\text{parameters}})]^{1/2}$ .

**Table 2** Selected bond distances ( $\text{\AA}$ ) and angles ( $^\circ$ ) for complexes **1** and **2**

	<b>1</b>	<b>2</b>
Mo(1)–Mo(1a)	2.127(4)	2.121(4)
Mo(2)–Mo(2a)	2.127(1)	2.123(1)
Mo(1)–Cl	2.440(5)	2.441(5)
Mo(2)–Cl	2.460(5)	2.457(5)
Mo(1)–N	2.221(14)	2.230(13)
Mo(2)–N	2.175(14)	2.142(13)
Cl–Mo(1)–N	87.4(4)	88.1(4)
Cl–Mo(1)–Mo(1a)	103.3(1)	103.3(1)
N–Mo(1)–Cl(a)	87.1(4)	88.1(4)
Cl–Mo(2)–Mo(2a)	102.1(1)	102.3(1)
Cl–Mo(2)–Cl(b)	155.8(2)	155.3(2)
N–Mo(2)–N(b)	150.5(8)	148.3(8)
N–Mo(1)–Mo(1a)	102.0(4)	100.5(3)
Cl–Mo(1)–Cl(a)	153.4(2)	153.3(2)
N–Mo(1)–N(a)	156.1(8)	159.0(7)
Cl–Mo(2)–N	88.0(4)	88.6(4)
N–Mo(2)–Mo(2a)	104.8(4)	105.8(4)
N–Mo(2)–Cl(b)	85.9(4)	84.7(4)

**Fig. 3** An ORTEP drawing showing both of the primary and secondary forms of  $[\text{Mo}_2\text{Cl}_4(\text{S-chea})_4]$ 

the primary to the secondary form are 97:3 and 94:6 for **1** and **2**, respectively. The primary form of complex **1** is twisted about the Mo–Mo bond with an angle of  $6.5^\circ$  in a clockwise direction  $\{\Delta-[\text{Mo}_2\text{Cl}_4(\text{S-chea})_4], \Delta S, \mathbf{1p}\}$ . The secondary form was found to have a twist angle of  $3.9^\circ$  in a counterclockwise direction  $\{\Lambda-[\text{Mo}_2\text{Cl}_4(\text{S-chea})_4], \Delta S, \mathbf{1s}\}$ . The primary and secondary forms of complex **2** were found to have a twist angle of  $5.9^\circ$  in a

**Fig. 4** Absorption spectrum (—) of  $[\text{Mo}_2\text{Cl}_4(\text{S-chea})_4]$  and solution CD spectra of  $[\text{Mo}_2\text{Cl}_4(\text{S-chea})_4]$  (----) and  $[\text{Mo}_2\text{Cl}_4(\text{R-chea})_4]$  (—)**Fig. 5** Solid-state CD spectra of  $[\text{Mo}_2\text{Cl}_4(\text{S-chea})_4]$  (----) and  $[\text{Mo}_2\text{Cl}_4(\text{R-chea})_4]$  (—) as KBr discs

counterclockwise direction  $\{\Lambda-[\text{Mo}_2\text{Cl}_4(\text{R-chea})_4], \Delta R, \mathbf{2p}\}$  and of  $2.9^\circ$  in a clockwise direction  $\{\Delta-[\text{Mo}_2\text{Cl}_4(\text{R-chea})_4], \Delta R, \mathbf{2s}\}$ , respectively. The twists of complexes **1** and **2** are clearly due to the steric crowding of the ligands and the packing of the molecules in the crystals. The conformational preferences of the chiral ligands induces the preferable twist along the Mo–Mo bond. This contrasts with the  $\beta$ -form complexes where a staggered geometry is produced due to the ligand constraints of the bridging ligands. The Mo atoms of the chiral, bridged complexes  $\beta-[\text{Mo}_2\text{Cl}_4(\text{R,R-diop})_2]$  were also found to be disordered. The primary form, which has a  $\Lambda$  configuration, occupies 89% of the sites, while the secondary form ( $\Delta$  molecule) occupies the remaining 11%.<sup>5</sup> The differences in the populations of the two conformers of the enantiomeric complexes **1** and **2** in the crystals should be due to the packing force during crystallization. This is verified by the fact that the populations in the solid are different from those in solution (see below).

### Absorption and CD spectra

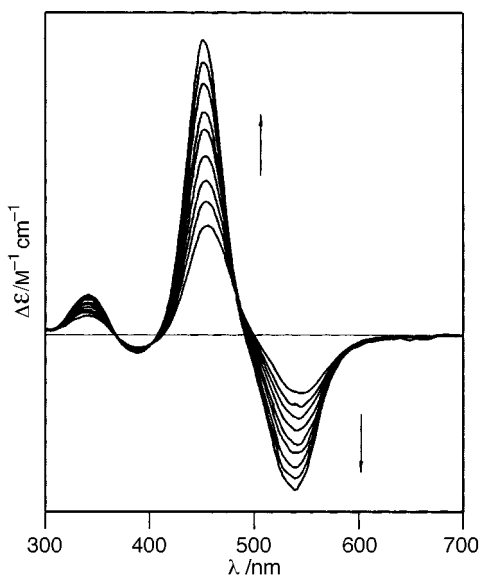
The absorption spectra (see Fig. 4 for a representative spectrum of **1**) of complexes **1** and **2** are similar and are typical for compounds with a Mo–Mo quadruple bond. The lowest-energy bands at 531 nm can be assigned to  $\delta_{xy} \rightarrow \delta_{xy}^*$  ( $\epsilon = 1647\text{ M}^{-1}\text{ cm}^{-1}$ ) transitions.<sup>4</sup> The second lowest-energy bands appear at 455 nm, which can most probably be assigned to the forbidden transition  $\delta_{xy} \rightarrow \delta_{x^2-y^2}$  ( $\epsilon = 250\text{ M}^{-1}\text{ cm}^{-1}$ ).<sup>4</sup>

Fig. 5 shows the solid-state CD spectra for complexes **1** and **2**, obtained by mulling crystals as KBr discs. Clearly there is a mirror-image relationship between the spectra of the enantiomeric molecules. The spectrum of **1** has a positive sign for the  $\delta_{xy} \rightarrow \delta_{xy}^*$  transition (520 nm) and a negative sign for the  $\delta_{xy} \rightarrow \delta_{x^2-y^2}$  transition (455 nm), while that of **2** has a negative sign for the  $\delta_{xy} \rightarrow \delta_{xy}^*$  transition and a positive sign for the  $\delta_{xy} \rightarrow \delta_{x^2-y^2}$  transition. The composition of an

**Table 3** The CD signs of  $\delta_{xy} \longrightarrow \delta_{xy}^*$  and  $\delta_{xy} \longrightarrow \delta_{x^2-y^2}$  transitions for complexes **1** and **2**

State	[Mo <sub>2</sub> Cl <sub>4</sub> (S- <i>chea</i> ) <sub>4</sub> ]		[Mo <sub>2</sub> Cl <sub>4</sub> (R- <i>chea</i> ) <sub>4</sub> ]	
	$\delta_{xy} \longrightarrow \delta_{xy}^*$	$\delta_{xy} \longrightarrow \delta_{x^2-y^2}$	$\delta_{xy} \longrightarrow \delta_{xy}^*$	$\delta_{xy} \longrightarrow \delta_{x^2-y^2}$
Crystal <sup>a</sup>	+	-	-	+
Powder <sup>b</sup>	+	-	-	+
Solution c <sup>c</sup>	-	+	+	-
Solution p <sup>d</sup>	-	+	+	-

<sup>a</sup> Spectrum obtained by pressing the crystals into a KBr disc. <sup>b</sup> Spectrum obtained by pressing the powder into a KBr disc. <sup>c</sup> Spectrum obtained by dissolving the crystals in toluene. <sup>d</sup> Spectrum obtained by dissolving the powder in toluene.

**Fig. 6** The CD spectra of [Mo<sub>2</sub>Cl<sub>4</sub>(S-*chea*)<sub>4</sub>] in toluene at -10, 0, +10, +25, +35, +50, +65, +80 and +100 °C. The arrows indicate decreasing temperature

observed CD band consists of the Cotton-effect contributions of all the species present. Since the ratios of the primary to the secondary form are 97:3 and 94:6 for **1** and **2**, respectively, in the crystals, the CD spectrum of **1** should show the optical activity of the  $\Delta$  form and that of **2** the optical activity of the  $\Lambda$  form. The positive phase of the CD spectrum of complex **1** and the negative phase of **2** for the  $\delta_{xy} \longrightarrow \delta_{xy}^*$  transitions are consistent with expectation according to the CD sign rule.<sup>3</sup> Opposite signs for the  $\delta_{xy} \longrightarrow \delta_{xy}^*$  and  $\delta_{xy} \longrightarrow \delta_{x^2-y^2}$  transitions have also been observed consistently in the past for phosphine complexes of the type Mo<sub>2</sub>X<sub>4</sub>(L-L)<sub>2</sub> and is expected theoretically.<sup>3</sup> Fig. 4 also shows the CD spectra of **1** and **2** in tetrahydrofuran (thf). The shapes of the spectra in solution are similar to those in the solid state except that the bands of the solution spectra at 400 nm are much weaker. Most interestingly, the solution CD spectra of complexes **1** and **2** show negative and positive phases for the  $\delta_{xy} \longrightarrow \delta_{xy}^*$  transitions, respectively, which are opposite to those found in the solid-state CD spectra. This indicates that the primary form of **1** in solution has a  $\Lambda$  configuration and that of **2** has a  $\Delta$  configuration. The  $\Delta S \rightleftharpoons \Lambda S$  (or  $\Lambda R \rightleftharpoons \Delta R$ ) isomerization reactions occur upon dissolution of the crystals in thf. The interchange is possible since the monodentate amine ligands have no ligand constraint to limit the rotation of the metal-metal bond. Table 3 lists the CD signs of the  $\delta_{xy} \longrightarrow \delta_{xy}^*$  and  $\delta_{xy} \longrightarrow \delta_{x^2-y^2}$  transitions of complexes **1** and **2** in solution and in the solid state.

To study the  $\Delta S \rightleftharpoons \Lambda S$  and  $\Lambda R \rightleftharpoons \Delta R$  isomerization reactions the variable-temperature CD spectra were measured. When the spectra of complexes **1** and **2** were measured in the solid state no change was observed from -10 to 100 °C. This

indicates that at this accessible temperature range the energy is not large enough for the molecules to isomerize in the solid state. However, when the spectra were measured in toluene solutions significant variations were detected. The CD spectra of both complexes intersect in isosbestic points, indicating temperature-dependent equilibria between pairs of conformers.<sup>18</sup> Fig. 6 shows representative temperature-dependent CD spectra for **1**. Both the CD peaks corresponding to the  $\delta_{xy} \longrightarrow \delta_{xy}^*$  and  $\delta_{xy} \longrightarrow \delta_{x^2-y^2}$  transitions show a uniform decrease with increasing temperature, denoting a smaller population difference of the two conformers at higher temperature. It is also noted that the isomerizations are reversible. Each CD transition was able to return to its absorption intensity at the starting temperature.

The temperature-dependent CD spectra of complexes **1** and **2** provide a unique opportunity to study the free energy change of the  $\Delta S \rightleftharpoons \Lambda S$  and  $\Lambda R \rightleftharpoons \Delta R$  isomerization reactions of a quadruply bonded complex and the Wood-Fickett-Kirkwood (WFK) method<sup>18-20</sup> is invoked for this purpose. If a system containing two components in thermal equilibrium displays a measurable intensity parameter  $A_{\text{obs}}$ , which is the population-weighted sum of the temperature-independent values  $A_1$  and  $A_2$  of the two conformers in either complex **1** or **2**, it is possible to evaluate  $A_1$  and  $A_2$  from measurement of  $A_{\text{obs}}$  over a wide temperature range. The expression which relates  $A_{\text{obs}}$  to  $A_1$  and  $A_2$  is  $A_{\text{obs}} = (A_1 - A_2)[1 + \exp(-\Delta G_{12}^\circ/RT)]^{-1} + A_2$ , where  $\Delta G_{12}^\circ$  is the standard Gibbs free-energy change for the  $\Delta S \rightleftharpoons \Lambda S$  or  $\Lambda R \rightleftharpoons \Delta R$  isomerization reaction,  $R$  the gas constant and  $T$  the temperature. The correct  $\Delta G_{12}^\circ$  value is the one which makes the  $A_{\text{obs}}$  and  $[1 + \exp(-\Delta G_{12}^\circ/RT)]^{-1}$  relation linear. We have applied this method of conformational analysis to complexes **1** and **2** in toluene based on the  $\Delta \epsilon$  values<sup>18</sup> of the  $\delta_{xy} \longrightarrow \delta_{xy}^*$  and  $\delta_{xy} \longrightarrow \delta_{x^2-y^2}$  transitions. A linear relationship between  $\Delta \epsilon$  and  $[1 + \exp(-\Delta G_{12}^\circ/RT)]^{-1}$  could be found for  $\Delta G_{12}^\circ$  values in the range from 0.8 to 1.0 kcal mol<sup>-1</sup>. The free energy change for the  $\Delta \rightleftharpoons \Lambda$  isomerization is thus taken as  $\Delta G_{12}^\circ = 0.19 \pm 0.1$  kcal mol<sup>-1</sup>. On the basis of the equation for the equilibrium constant  $K$ ,  $K = \exp(-\Delta G_{12}^\circ/RT) = P_2/P_1$  where  $P_1$  and  $P_2$  are the populations of the two conformers, the populations of the conformers at 25 °C are calculated as  $82 \pm 2\%$  for the major isomer and  $18 \pm 2\%$  for the minor one. The populations at +100 °C are  $77 \pm 3$  and  $23 \pm 3\%$ , respectively. The dissymmetry ( $g = \Delta \epsilon/\epsilon$ ) factors for the  $\delta_{xy} \longrightarrow \delta_{xy}^*$  and  $\delta_{xy} \longrightarrow \delta_{x^2-y^2}$  transitions of complex **1** are thus calculated as  $-4.7 \times 10^{-3}$  and  $4.0 \times 10^{-2}$ , respectively. Those of **2** are  $6.4 \times 10^{-3}$  and  $-5.2 \times 10^{-2}$ , respectively. It is noted that the population difference in solution is smaller than that in the solid state. This is expected since in solution there is no packing force that limits the isomerization of the conformers. Although the  $\Delta G_{12}^\circ$  value is small and might lead to low precision of the results,<sup>18</sup> the conformational analysis by the WFK method predicts that in toluene solution the complexes  $\Delta S$  and  $\Lambda R$  are more stable than their corresponding conformers  $\Lambda S$  and  $\Delta R$  by  $0.9 \pm 0.1$  kcal mol<sup>-1</sup>. This is the first reported value of a free-energy change for the  $\Delta \rightleftharpoons \Lambda$  isomerization of quadruply bonded complexes.

## NMR spectra

The two-dimensional  $^{15}\text{N}$ - $^1\text{H}$  HMQC (heteronuclear multiple quantum coherence) spectrum for complex **1** in  $\text{CDCl}_3$  shows that the two protons centered at  $\delta$  4.51 and 3.60 are correlated with the  $^{15}\text{N}$  atom and can be assigned to the two H protons bonded to the nitrogen atom. The other peaks in the  $^1\text{H}$  NMR spectrum were well separated and can be assigned as follows:  $\delta$  2.98 (1 H, CH) and 1.00–1.75 (11 H, cyclohexyl). The chemical shift of the  $^{15}\text{N}$  atom is  $\delta$   $-337.58$  and  $^1J_{\text{NH}}$  is about 68 Hz. It is noted that although NMR spectroscopic studies often give detailed information about the components in an equilibrium mixture of isomers, the variable-temperature  $^1\text{H}$  NMR spectra of complexes **1** and **2** in  $\text{CDCl}_3$  or  $\text{CD}_2\text{Cl}_2$  displayed no broadenings or splittings at temperatures from 50 to  $-80$  °C. This indicates that the barrier separating the rotamers is not high enough to allow observation of their resolved spectra in the accessible temperature region.

## Conclusion

The syntheses of the first quadruply bonded complexes containing chiral, monodentate amine ligands have been successfully accomplished and their structures determined. These complexes show opposite configurations for the core structures in crystals to those in solution. The populations of the conformers in solution are also different from those in the solid. This contrasts with the bridging complex  $\beta$ - $[\text{Mo}_2\text{Cl}_4(\text{R},\text{R}\text{-diop})_2]$  where the configuration of the conformer in the crystal was retained in solution, although the ratios of the two conformers in solid and in solution were not the same.<sup>5</sup> To our knowledge, this is the first time a complete switch in CD signs has been observed in this type of complex. We have also shown that although NMR techniques in many investigations produce as clear information about the conformations of complexes as does the CD method, the latter is more beneficial in cases where the rotation barrier is low. It was reported that NMR techniques have failed for many organic compounds where the barrier to exchange is below  $6 \text{ kcal mol}^{-1}$ .<sup>18</sup>

## Acknowledgements

We are grateful to the National Science Council of the Republic of China for support. We also thank Ms. Shou-Ling Huang of the National Taiwan University for the variable-temperature NMR study.

## References

- 1 F. A. Cotton and R. A. Walton, *Multiple Bonds between Metal Atoms*, Oxford University Press, London, 2nd edn., 1993.
- 2 A. Moscovitz, *Tetrahedron*, 1961, **13**, 48.
- 3 R. D. Peacock, *Polyhedron*, 1987, **6**, 715.
- 4 P. A. Agaskar, F. A. Cotton, I. F. Fraser, M. M. Ljubica, K. W. Muir and R. D. Peacock, *Inorg. Chem.*, 1986, **25**, 2511.
- 5 J.-D. Chen, F. A. Cotton and R. L. Falvello, *J. Am. Chem. Soc.*, 1990, **112**, 1076.
- 6 J.-D. Chen and F. A. Cotton, *Inorg. Chem.*, 1990, **29**, 1797.
- 7 J.-D. Chen and F. A. Cotton, *J. Am. Chem. Soc.*, 1991, **113**, 2509.
- 8 C.-T. Lee, J.-D. Chen, Y. W. Chen-Yang, L.-S. Liou and J.-C. Wang, *Polyhedron*, 1997, **16**, 473.
- 9 I. F. Fraser and R. D. Peacock, *Inorg. Chem.*, 1985, **24**, 988.
- 10 I. F. Fraser, A. McVitie and R. D. Peacock, *Polyhedron*, 1986, **5**, 39.
- 11 M. Gerards, *Inorg. Chim. Acta*, 1995, **229**, 101.
- 12 R. N. McGinnis, T. R. Ryan and R. E. McCarley, *J. Am. Chem. Soc.*, 1978, **100**, 7900.
- 13 SMART/SAINT/ASTRO, Release 4.03, Siemens Energy & Automation, Inc., Madison, WI, 1995.
- 14 G. M. Sheldrick, SHELXTL PLUS, Release 4.1, Siemens Analytical X-Ray Instruments Inc., Karlsruhe, 1991.
- 15 F. A. Cotton, M. W. Extine, T. R. Felthouse, B. W. S. Kolthammer and D. G. Lay, *J. Am. Chem. Soc.*, 1981, **103**, 4040.
- 16 C. K. Johnson, ORTEP, Report ORNL-5138, Oak Ridge National Laboratory, Oak Ridge, TN, 1976.
- 17 F. A. Cotton and R. Poli, *J. Am. Chem. Soc.*, 1988, **110**, 830.
- 18 K. Nakanishi, N. Berova and R. W. Woody, *Circular Dichroism: Principles and Applications*, VCH, Weinheim, 1994.
- 19 W. W. Wood, W. Fickett and J. G. Kirkwood, *J. Chem. Phys.*, 1952, **20**, 561.
- 20 A. Moscovitz, K. M. Wellman and C. Djerassi, *J. Am. Chem. Soc.*, 1963, **85**, 3515.

Received 4th July 1997; Paper 7/04751G